



## Microstructures and magnetic properties of carbon nanotube/Co-oxide nanocomposite powders

Kyung Tae Kim<sup>a,\*</sup>, Gook Hyun Ha<sup>a</sup>, Jürgen Eckert<sup>b,c</sup>

<sup>a</sup> Korea Institute of Materials Science, Functional Materials Division, 797 Changwon-daero, Changwon, Gyeongnam 641-831, Republic of Korea

<sup>b</sup> IFW Dresden, Institute for Complex Materials, P.O. BOX 27 01 16, D-01171 Dresden, Germany

<sup>c</sup> Institute of Materials Science, TU Dresden, D-01062 Dresden, Germany

### ARTICLE INFO

#### Article history:

Received 2 July 2010

Received in revised form 9 December 2010

Accepted 5 January 2011

Available online 12 January 2011

#### Keywords:

Nanocomposite  
Carbon nanotube  
Co oxide  
Microstructure

### ABSTRACT

Carbon nanotube embedded cobalt oxide (CNT/Co-oxide) nanocomposite powders were synthesized by molecular-level mixing followed by calcination. The surface morphology of the fabricated nanocomposite powders shows Co-oxide coated CNTs homogeneously dispersed in the Co-oxide nanopowders. XRD patterns reveal that CoO–Co<sub>3</sub>O<sub>4</sub> nanopowders were obtained as a complex phase. The nanocomposite powders exhibit ferromagnetism with a saturation magnetization of 75 emu g<sup>-1</sup>, while CoO–Co<sub>3</sub>O<sub>4</sub> nanopowders without CNTs are paramagnetic. These results indicate that incorporating CNTs into Co-oxide nanopowders triggers a change of the magnetic properties towards ferromagnetism.

© 2011 Elsevier B.V. All rights reserved.

### 1. Introduction

Incorporating carbon nanotubes (CNTs) into inorganic matrices such as metals and ceramics has attracted much attention in structural and multi-functional applications due to their superior mechanical, electrical and thermal properties [1]. There have been several meaningful progresses [2–6] in CNT-reinforced ceramic and metal matrix (CNT/ceramic, CNT/metal) composites. For example, Zhan et al. [2] found a highly enhanced toughness of Al<sub>2</sub>O<sub>3</sub> by CNT addition and Peigney et al. [3] reported a novel fabrication process for CNT/Al<sub>2</sub>O<sub>3</sub> nanocomposite powders with high surface area and improved mechanical properties. Cha et al. [5] showed both enhanced toughness and hardness by CNT addition, simultaneously. Till date, most of the research has been focused on improving the mechanical properties of CNT/ceramic composites [2–4], some of them are also studied for use as electronic conductors or thermoelectric materials [7]. However, there are only limited reports on the magnetic properties of CNT/ceramic composites [8,9] because of the problem of severe agglomeration of CNTs in the inorganic matrix the problems associated with the usually employed powder metallurgy processing have not been efficiently solved, yet. However, the

recently developed fabrication process of mixing metal salts and functionalized CNTs at the molecular level [10] is promising to allow for a homogeneous dispersion of CNTs in ceramic matrix materials.

Here, we report on the fabrication and the magnetic properties of CNT/Co-oxide nanocomposite powders in which CNTs surrounded by a Co-oxide shell are well mixed in nano-sized Co-oxide particles. Pure Co oxide material without CNTs was also fabricated under the same conditions such as to elucidate the effect of CNT addition. We find that the paramagnetic behavior of Co-oxide materials is changed into ferromagnetic behavior by addition of CNTs. This transformation of the magnetic properties by addition of CNTs may be described by Co clustering concept and disordered spin states near the CNT/Co oxide interface.

### 2. Experimental procedure

Multi-walled CNTs (95% purity) synthesized by thermal chemical vapor deposition were used as reinforcements for the CNT/Co-oxide nanocomposite powders. The CNTs were cleansed for 24 h in HF solution, and then functionalized in a mixed solution of H<sub>2</sub>SO<sub>4</sub>/HNO<sub>3</sub> (3:1 ratio) to attach carboxyl groups or carbonyl groups on the CNT surface. The functionalized CNTs were dispersed within 500 ml ethanol solvent via ultrasonic treatment for 30 min to form a stable suspension. Cobalt nitrate hexahydrate (99.995%, 6H<sub>2</sub>O(NO<sub>3</sub>)<sub>2</sub>Co) was added to the CNT suspension and treated in an ultrasonic bath for 30 min. Thermogravimetric analysis (TGA) of the Co nitrate salt was performed to obtain the temperature for calcination. The solution mixed at the molecular level [10] was vaporized with magnetic stirring at 373 K; the dried powders were subsequently calcinated for 5 min at 553 K in air. The phase analysis of the calcinated Co-oxide powders was done by X-ray powder diffraction (XRD) using a X'pert MPD 3040 diffractometer with Cu K $\alpha$  radiation. The weight percent of CNTs was obtained from elemental analysis (EA1110-FISONS) of the CNT/Co-oxide

\* Corresponding author at: Korea Institute of Materials Science, Functional Materials Division, 66 Sangnam-dong, Changwon 641-831, Republic of Korea. Tel.: +82 55 280 3506; fax: +82 55 280 3392.

E-mail address: [ktkim@kims.re.kr](mailto:ktkim@kims.re.kr) (K.T. Kim).

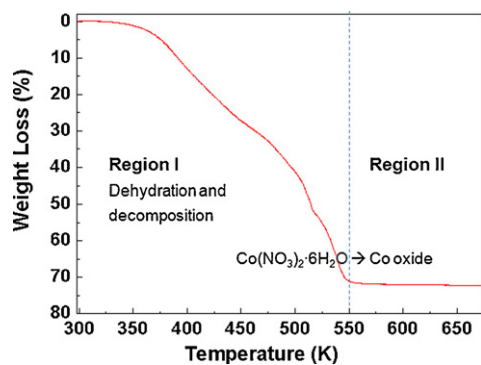


Fig. 1. TGA results for Co nitrate hydrate at a heating rate of  $5 \text{ K min}^{-1}$ .

composite powders. The surface morphology and composition of the nanocomposite powders were characterized by field emission scanning electron microscopy (FE-SEM, MIRA||LMH, TESCAN). The chemical bonding between the CNTs and the Co-oxide matrix was investigated by FT-IR analysis of the nanocomposite powders. The magnetic properties of the nanocomposite powders were characterized by using a vibrating sample magnetometer (Riken Denshi Co. Ltd.).

### 3. Results and discussion

Fig. 1 shows the TGA result of Co nitrate hexahydrate with increasing temperature from 298 to 673 K in air. A high weight loss as indicated in Fig. 1 was observed in Region I which spans between 298 and 548 K. We expect that the Co salts are dehydrated and decomposed vigorously in this temperature range. In fact, the weight loss of 72% observed for the temperature regime between 298 and 548 K corresponds to the theoretically calculated

value when  $\text{Co}(\text{NO}_3)_2 \cdot 6\text{H}_2\text{O}$  is transformed into the Co oxide phase. It is believed that the Co-oxide phase formed in Region I could be stabilized into CoO or  $\text{Co}_3\text{O}_4$ , respectively.

Fig. 2(a) shows the morphology of the CNT/Co-oxide nanocomposite powders in which CNTs seem to be coated with Co-oxide nanomaterial. The coated CNTs-like core-shell structure is well mixed in the Co-oxide powder. The enlarged FE-SEM image of an individual CNT surrounded by Co-oxide nanopowders shown in Fig. 2(b) reveals a nano-wire microstructure with 200 nm diameter. The surface morphology of Co-oxide nanopowders synthesized without CNTs is displayed in Fig. 2(c). The X-ray diffraction pattern in Fig. 2(d) confirms that the phase present in the synthesized Co-oxide nanopowders is a complex phase consisting of CoO matched with JCPDS no. 78-0431 and  $\text{Co}_3\text{O}_4$  matched with JCPDS no. 76-1802. These phases were observed simultaneously in the nanocomposite powders. On the other hand, during calcination of the nanocomposite powders mixing of CNTs with Co salt, chemical bonds between the CNTs and crystalline Co-oxide formed, as proved in Fig. 3. The strong peak observed nearby  $565 \text{ cm}^{-1}$  corresponds to the contribution from interfacial bonding between carbon atoms in the carbon nanotube and Co in the Co oxide. Another peak at  $665 \text{ cm}^{-1}$  shows clear bonding in the Co oxide material. The absorbance peaks for diamond ( $\text{sp}^3$ ) and graphite ( $\text{sp}^2$ ) in CNTs is revealed at wave numbers ranging from 1300 to  $1600 \text{ cm}^{-1}$ , respectively. These results reveal that the CNTs are present and dispersed in the nanocomposite powders even though no transmission electron microscopy investigations were performed to check the embedded CNTs.

The measured specific surface area of the fabricated CNT/Co-oxide nanocomposite powders is compared to that of Co oxide nanopowders fabricated by the same process in Fig. 4. The highest

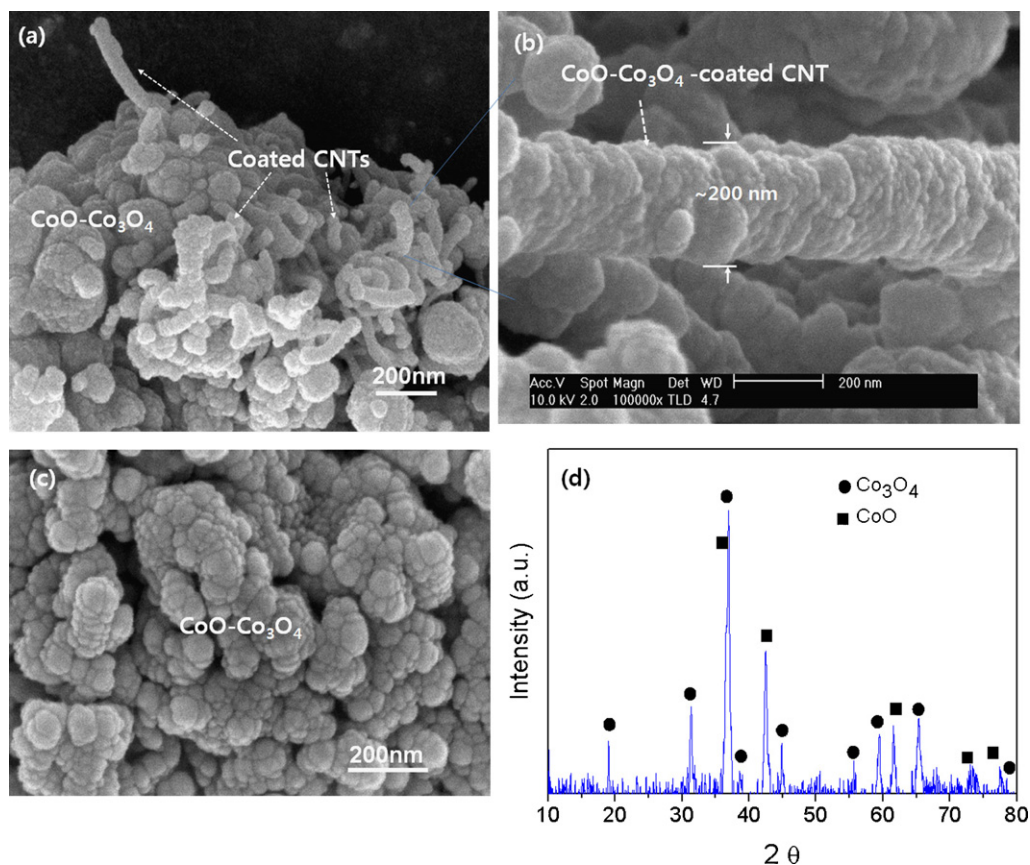


Fig. 2. (a) FE-SEM image of CNT/Co-oxide nanocomposite powder (b) enlarged morphology of the CNT/Co-oxide nanostructures in (a), (c) FE-SEM image of Co-oxide nanopowders, and (d) XRD patterns of the Co-oxide nanopowders ( $\text{Co}_3\text{O}_4$  and CoO is defined by JCPDS file no. 76-1802 and 78-0431, respectively).

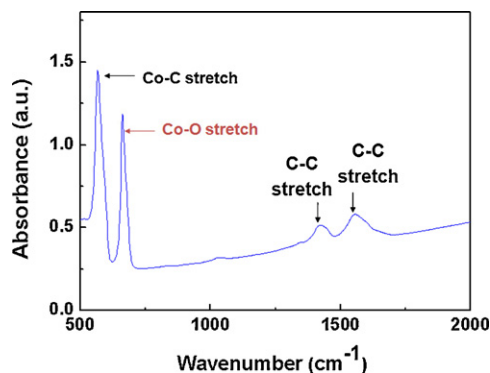


Fig. 3. FT-IR results of the CNT/Co-oxide nanocomposite powders.

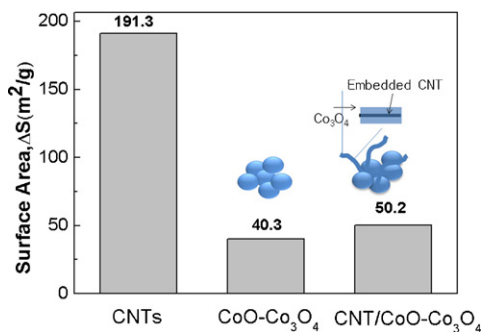


Fig. 4. Comparison of the measured specific surface area of CNTs, Co-oxide and CNT/Co-oxide nanocomposite powders. The depicted illustrations in the figure show the assembly of the Co-oxide and the nanocomposite powders, respectively.

surface area,  $191.3 \text{ m}^2/\text{g}$  was obtained for multi-walled CNTs which were purified and functionalized in this study. The CNT/Co oxide nanocomposite powders exhibit a slightly higher specific surface area of  $50.2 \text{ m}^2/\text{g}$  compared to  $40.3 \text{ m}^2/\text{g}$  of Co oxide nanopowders without CNTs. The surface area of the nanocomposite powders is not increased because they are perfectly coated even though CNTs are added.

Fig. 5 displays the  $M-H$  curve of functionalized CNTs showing weak ferromagnetic behavior with the saturation magnetization of  $3.8 \text{ emu g}^{-1}$  at 300 K. Most likely, the very weak ferromagnetic behavior of the CNTs comes from the small amount of remnant Co catalysts that was used to grow the CNTs in the thermal CVD chamber. As shown in Fig. 6, the  $M-H$  curve of Co oxide nanopowders at 300 K exhibits a linear paramagnetic behavior in the whole region of measurement. The fact that there are little coercivity means the proportion of CoO or  $\text{Co}_3\text{O}_4$  remaining paramagnetic

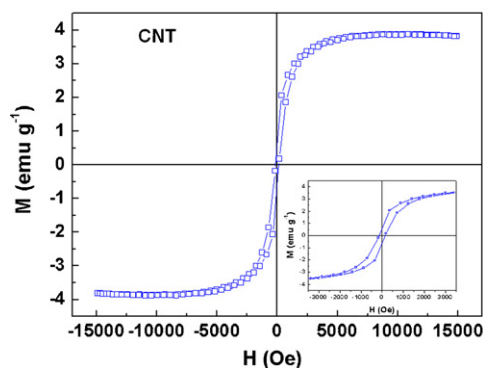


Fig. 5. Magnetization versus applied magnetic field ( $M-H$ ) curves for CNTs used in this study. The inset is magnified  $M-H$  hysteresis loop.

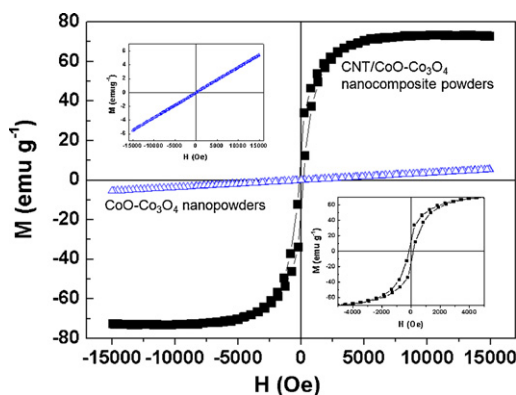


Fig. 6. Comparison of  $M-H$  hysteresis loops of the CoO- $\text{Co}_3\text{O}_4$  nanopowders and CNT/Co-oxide nanocomposite powders. The upper inset shows the magnified hysteresis loops of the CoO- $\text{Co}_3\text{O}_4$  nanopowders. The lower inset shows the magnified hysteresis loop of the nanocomposite powders.

state is much larger than that in antiferromagnetic state [11,12]. Fig. 6(b) also shows the  $M-H$  hysteresis loop of the 6 vol.% CNT/Co oxide nanocomposite powder at 300 K. Obviously, the nanocomposite powder exhibits ferromagnetic behavior while Co oxide nanopowders consisting of CoO and  $\text{Co}_3\text{O}_4$  phases clearly show paramagnetic properties and a 20 times higher saturation magnetization,  $75 \text{ emu g}^{-1}$  than that of the CNTs, which are also rather weakly ferromagnetic (see inset in Fig. 5). These results show that the magnetic behavior of complex Co oxide changes from paramagnetism to ferromagnetism but also the saturation magnetization shows high value,  $75 \text{ emu g}^{-1}$  compared to other Co oxide nanomaterials by addition of 6 vol.% CNTs.

Based on our fabrication process to produce the nanocomposite powders, it is deduced that the transformation of magnetic properties of Co oxide materials by addition of CNTs comes from ferromagnetic CNTs embedded in the paramagnetic materials and the high saturation magnetization originates from the functionalized CNT/Co-oxide interface, where Co clustering present at the atomic scale due to the chemically bonded interface between carbon and Co atoms, as indicated in Fig. 2. That is, since purified CNTs used in this study have many oxygen-containing functional groups on the surface [6], Co ions or Co atoms might be locally concentrated near functional groups and homogeneously dispersed on the CNT surface in atomic scale. Hence, we think this kind of CNT/Co-oxide interface can maximize the effect of uncompensated surface spins on the Co-oxide nanopowders system that results in ferromagnetism. Similar ferromagnetic behavior by addition of CNTs also previously observed in the CNT/CoO nanostructure system where it is described that its magnetic performance is attributed the uncompensated surface spin states or ferromagnetic Co clusters [9,13].

#### 4. Conclusions

CNT/Co-oxide nanocomposite powders were fabricated by molecular-level mixing followed by calcination. The chemical bonding between the functionalized CNTs and Co oxide creates a characteristic microstructure of Co oxide-coated CNTs dispersed among the  $\text{Co}_3\text{O}_4$  nanoparticles. The nanocomposite powders exhibit a transition of the magnetic properties from the paramagnetism of Co oxide to weak ferromagnetism due to addition of ferromagnetic CNTs. The highly enhanced saturation magnetization of the nanocomposite powders compared to that of CNTs may be explained by uncompensated spin states at the chemically bonded interface between Co clusters on the CNT surface and Co oxide. These results indicate that incorporating CNTs into Co-oxide

nanopowders changes the physical properties of the material due to the synergistic effect between CNTs and oxide nanopowders.

### Acknowledgement

This study was supported by the Fundamental R&D Program for Core Technology of Materials funded by the Ministry of Knowledge Economy (MKE), Republic of Korea.

### References

- [1] P.J.F. Harris, *Int. Mater. Rev.* 49 (1) (2004) 31–43.
- [2] G.-D. Zhan, J.D. Kuntz, Wan Julin, A.K. Murkherjee, *Nat. Mater.* 2 (2003) 38–42.
- [3] A. Peigney, E. Flahaut, Ch. Laurent, F. Chastel, A. Rosset, *Chem. Phys. Lett.* 352 (2002) 20–25.
- [4] C.B. Mo, S.I. Cha, K.T. Kim, K.H. Lee, S.H. Hong, *Mater. Sci. Eng. A395* (2005) 124–128.
- [5] S.I. Cha, K.T. Kim, S.N. Arshad, C.B. Mo, S.H. Hong, *Adv. Mater.* 17 (2005) 1377–1381.
- [6] K.T. Kim, S.I. Cha, T. Gemming, J. Eckert, S.H. Hong, *Small* 4 (2008) 1936–1940.
- [7] L.D. Zhao, B. Zhang, J. Li, M. Zhou, W. Liu, J. Liu, *J. Alloys Compd.* 455 (2008) 259–264.
- [8] Z.Y. Sun, H.Q. Yuan, Z.M. Liu, B.X. Han, X.R. Zhang, *Adv. Mater.* 17 (2005) 2993–2997.
- [9] H. Zhang, N. Du, P. Wu, B. Chen, D. Yang, *Nanotechnology* 19 (2008) (art. No. 315604).
- [10] S.I. Cha, K.T. Kim, K.H. Lee, C.B. Mo, S.H. Hong, *Scripta Mater.* 53 (2005) 793–797.
- [11] L. Meng, W. Chen, C. Chen, *Chin. Phys. Lett.* 27 (2010) 128101.
- [12] J. Ma, S. Zhang, W. Liu, Y. Zhao, *J. Alloys Compd.* 490 (2010) 647–651.
- [13] H.T. Zhang, M. Han, Z.Y. Jiang, Y. Song, Z.X. Xie, Z. Xu, L.S. Zheng, *Chem. Phys. Chem.* 8 (2007) 2091–2095.